



**HAL**  
open science

## Evidence for a spin-lattice relaxation process with two optical phonons: $Mn^{2+}$ in ZnS

G. Roger, C. More, C. Blanc

► **To cite this version:**

G. Roger, C. More, C. Blanc. Evidence for a spin-lattice relaxation process with two optical phonons:  $Mn^{2+}$  in ZnS. *Journal de Physique*, 1980, 41 (2), pp.169-175. 10.1051/jphys:01980004102016900 . jpa-00209230

**HAL Id: jpa-00209230**

**<https://hal.science/jpa-00209230>**

Submitted on 4 Feb 2008

**HAL** is a multi-disciplinary open access archive for the deposit and dissemination of scientific research documents, whether they are published or not. The documents may come from teaching and research institutions in France or abroad, or from public or private research centers.

L'archive ouverte pluridisciplinaire **HAL**, est destinée au dépôt et à la diffusion de documents scientifiques de niveau recherche, publiés ou non, émanant des établissements d'enseignement et de recherche français ou étrangers, des laboratoires publics ou privés.

Classification  
 Physics Abstracts  
 76.30F

## Evidence for a spin-lattice relaxation process with two optical phonons : $Mn^{2+}$ in ZnS

G. Roger, C. More and C. Blanc

Université de Provence, Département d'Electronique (\*), 13397 Marseille Cedex 4, France

(Reçu le 9 juillet 1979, révisé le 1<sup>er</sup> octobre 1979, accepté le 18 octobre 1979)

**Résumé.** — On a étudié la relaxation spin-réseau de  $Mn^{2+}$  dans le ZnS cubique à 9 375 MHz entre 80 K et 900 K en mesurant l'élargissement de la transition  $|1/2\ 1/2\rangle \rightarrow |1/2\ -\ 1/2\rangle$ . Cette étude nous a montré que le temps de relaxation spin-réseau  $T_1$  mesuré à hautes températures ( $T > 273$  K) est de la forme

$$T_1^{-1} = \alpha T^7 I_6\left(\frac{\theta_D}{T}\right) + \beta \left[ \text{sh}^2 \frac{\theta_0}{T} \right]^{-1}.$$

Le premier terme correspond à un processus Raman dû aux phonons acoustiques, le deuxième fait intervenir des phonons optiques. Le calcul des probabilités de transition montre que les contributions des phonons optiques et acoustiques sont comparables.

**Abstract.** — We have studied the spin-lattice relaxation behaviour of  $Mn^{2+}$  in cubic ZnS at 9 375 MHz between 80 K and 900 K by measuring the line broadening of the  $|1/2\ 1/2\rangle \rightarrow |1/2\ -\ 1/2\rangle$  transition. This study shows that for high temperatures ( $T > 273$  K) the measured spin-lattice relaxation time  $T_1$  varies as

$$T_1^{-1} = \alpha T^7 I_6\left(\frac{\theta_D}{T}\right) + \beta \left[ \text{sh}^2 \frac{\theta_0}{T} \right]^{-1}.$$

The first term corresponds to a Raman process associated with the acoustical phonons, the second one arises from the optical phonons distribution. The transition probabilities calculation shows that the contributions from the optical and acoustical phonons are similar.

1. **Introduction.** — Wagner *et al.* [1] and Deville *et al.* [2, 3, 4, 5] have shown that when the temperature is higher than 25 K a single relaxation time  $T_1$  accounts for the spin-lattice relaxation of  $Mn^{2+}$  in ZnS. They explained the variation of  $T_1$  with temperature by a Raman process involving acoustical phonons only.

Deville's measurements were performed for  $T < 273$  K and lead, in the Raman region to the following law :

$$T_1^{-1} = 8.8 \times 10^{-10} T^7 I_6\left(\frac{\theta_D}{T}\right) \quad (T_1 \text{ s, } T \text{ K}) \quad (1)$$

with

$$\theta_D = 168 \text{ K} \quad \text{and} \quad I_6(x) = \int_0^x e^\omega (e^\omega - 1)^{-2} \omega^6 d\omega.$$

We present in section 2 results of determination of

$T_1$  from the variation of the E.P.R. linewidth for  $|1/2\ 1/2\rangle \rightarrow |1/2\ -\ 1/2\rangle$  transition in the temperature range 80-900 K. The relaxation law we deduce, shows a departure from the behaviour extrapolated from the law (1) deduced at lower temperature.

In section 3, we show that if we take into account Raman processes involving a narrow band of optical phonons then there appears in the expression for  $T_1^{-1}$  an extra term of the form

$$\beta \left[ \text{sh}^2 \frac{\theta_0}{T} \right]^{-1}. \quad (2)$$

Between 80 and 900 K the experimental values of  $T_1$  are best fitted by the following expression

$$T_1^{-1} = 8.8 \times 10^{-10} T^7 I_6\left(\frac{168}{T}\right) + 0.5 \times 10^6 \left[ \text{sh}^2 \frac{213}{T} \right]^{-1}.$$

(\*) Equipe de Recherche Associée au C.N.R.S. (E.R.A. 070375).

These  $\beta$  and  $\theta_0$  values are in agreement with our calculations made in section 3.

**2. Experimental results.** — Measurements were performed on a ZnS crystal ( $10^{-4}$  Mn<sup>2+</sup>/Zn concentration, cubic structure) with static field  $H_0$  parallel to the [001] axis, and on powder samples whose concentrations are  $10^{-4}$ ,  $10^{-5}$  and  $10^{-6}$ .

The spectrometer, made in our laboratory, is of classical design (homodyne detection at 9 375 MHz, magnetic field modulation at 100 kHz, klystron frequency locked on the measuring cavity); the absorption derivative  $d\chi''/dH$  was recorded.

Gaseous nitrogen flowing in a stainless steel worm used as a heating resistor and then guided by a quartz pipe set axially in the cylindrical cavity (TE<sub>011</sub> mode,  $Q_{\text{unloaded}} = 15\,000$ ) was used to heat the sample.

The gas temperature was measured before and after each recording using a thermocouple located in the same place as the sample. It was found to be constant to within 1 K for each recording. Thermal exchanges between the cavity and the nitrogen stream did not affect the  $Q$  value or the coupling of the cavity in any noticeable way. In the range 80 to 900 K, the recorded E.P.R. lines were lorentzian derivatives, so that an absorption line model resulting from the convolu-

tion of independent lorentzian spin packets with a lorentzian envelope was adopted. At 80 K, the peak-to-peak width of the recorded lines was 0.45 G for the  $10^{-4}$  doped samples and 0.32 G for the  $10^{-5}$  and  $10^{-6}$  doped samples. For a dipolar broadening, the widths of the spin packets are estimated to be 0.41 G, 0.04 G and 0.004 G for the  $10^{-4}$ ,  $10^{-5}$  and  $10^{-6}$  concentration respectively. This shows that the inhomogeneous broadening is about 0.3 G.

Furthermore, for all samples used, the peak to peak line width was constant from 80 K to 180 K and increased for higher temperatures. We have plotted in figure 1, in function of the temperature, the quantity  $D^{-1}$  (s<sup>-1</sup>) which shows the absorption line broadening caused by spin-lattice interactions; for all the data collected from 150 K to 900 K :

$$D^{-1} = \sqrt{\frac{3}{4}} \gamma (\Delta H_{\text{pp}}^* - \Delta H_{\text{R}}).$$

In this expression  $\gamma$  is the gyromagnetic ratio,  $H_{\text{pp}}^*$  the peak to peak line width for the temperature  $T$  and  $\Delta H_{\text{R}}$  the peak to peak width at low temperature.  $\Delta H_{\text{pp}}^* - \Delta H_{\text{R}}$  is thus the extra width due to spin-lattice relaxation and the quantity  $D$  is equal to  $T_1$  [6].

In the same figure, we have plotted the curve cor-

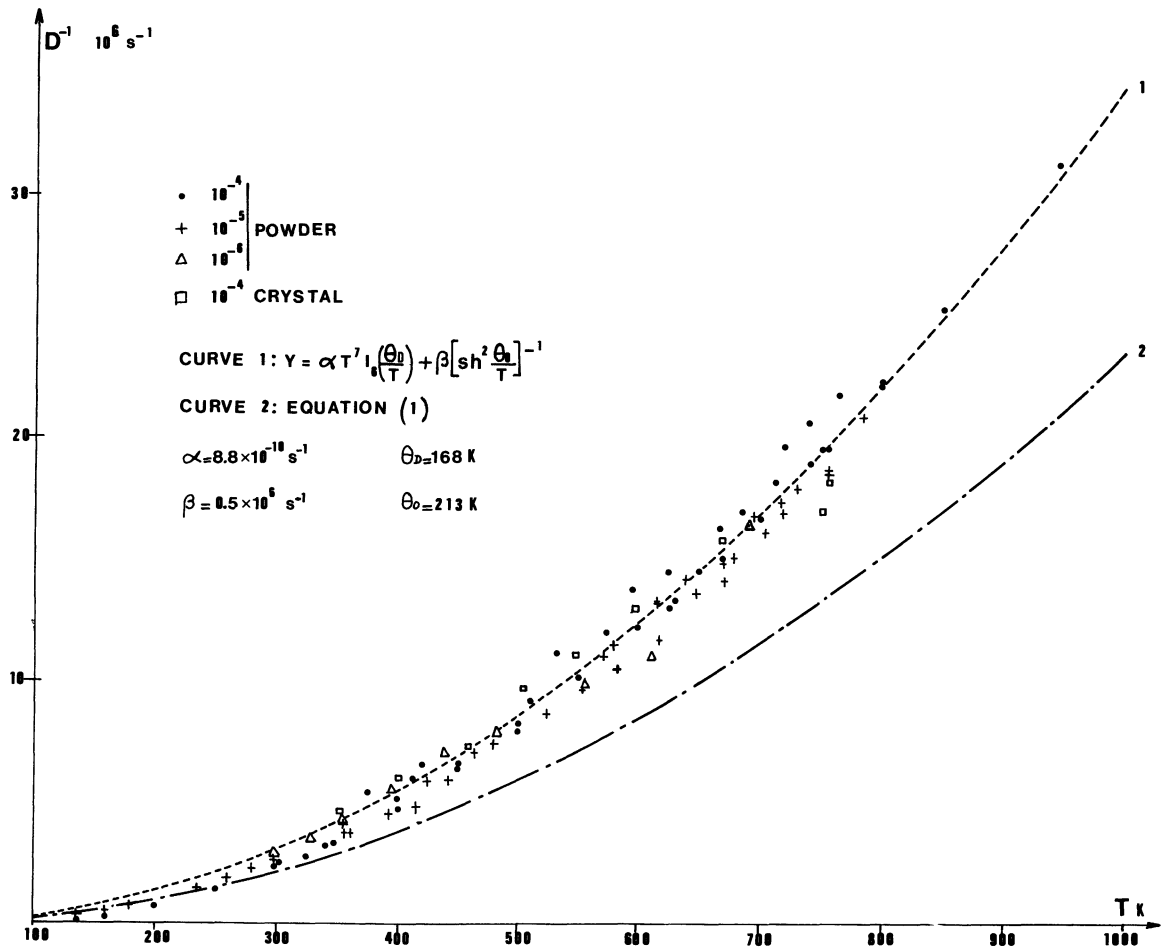


Fig. 1. — Experimental results and theoretical curves (see text).

responding to eq. (1) which accounts for the acoustical phonon Raman process. It can be seen that this process cannot explain by itself the broadening observed at high temperatures.

We show in section 3 that the new relaxation process thus revealed is due to optical phonons. We shall establish in fact that the contribution to the Raman process of the optical phonon branches takes the form  $\beta \left[ \text{sh}^2 \frac{\theta_0}{T} \right]^{-1}$ . Our experimental results lead to  $\beta = 0.5 \times 10^6 \text{ s}^{-1}$  and  $\theta_0 = 213 \text{ K}$ . The calculations show that  $2k\theta_0$  is a characteristic energy for the optical phonon branches involved. This  $\theta_0$  value determined from our measurements is in excellent agreement with Kunc's calculations [7] and with experimental values quoted in his work.

We shall show also that the contribution of the optical and acoustical phonons are of the same importance in the high temperature range which is in accordance with our experimental data.

**3. Interpretation.** — The life time of  $|^6A_1, M_S\rangle$  states is dependent upon the relaxation phenomena among these levels. Reciprocals of spin-lattice relaxation characteristic times are proportional to expressions linearly dependent upon probabilities  $W_{M_S \rightarrow M_S - K}$  for transitions  $|^6A_1 M_S\rangle \rightarrow |^6A_1 M_S - K\rangle$ . We aim to compare the efficiency of relaxation caused by two acoustical phonons and that by two optical phonons (Raman processes) when the temperature is high.

Optical phonons have already been shown to play a significant part in some instances [8, 9, 10]. On the other hand, the Raman process for  $Mn^{2+}$  in ZnS has been studied in detail at low temperatures [2, 3, 4, 5] and the experimental results follow the law (1). In previous works [2, 3, 4, 5] the lattice was approximately described as a Bravais lattice.

The occurrence of optical phonons necessitates the consideration of the real case of a lattice with a two atoms unit cell. The lattice is then generated by the vectors  $(\mathbf{a}_1, \mathbf{a}_2, \mathbf{a}_3)$  of a cell occupied by a Zinc atom at its origin (or Zn replaced by Mn without modifying the vibrations) and a sulfur atom set at

$$\mathbf{X}(S) = \frac{1}{4}(\mathbf{a}_1 + \mathbf{a}_2 + \mathbf{a}_3) \quad (\text{see Fig. 2}).$$

Taking a Zn atom as origin [11] the position of an atomic site is :

$$\mathbf{x}(l, \kappa) = \mathbf{x}(l) + \mathbf{X}(\kappa)$$

where

$$\mathbf{x}(l) = l_1 \mathbf{a}_1 + l_2 \mathbf{a}_2 + l_3 \mathbf{a}_3$$

and

$$\mathbf{X}(\kappa) = \begin{cases} 0 & \text{if } \kappa \equiv \text{Zn} \\ \mathbf{X}(S) & \text{if } \kappa \equiv \text{S} . \end{cases}$$

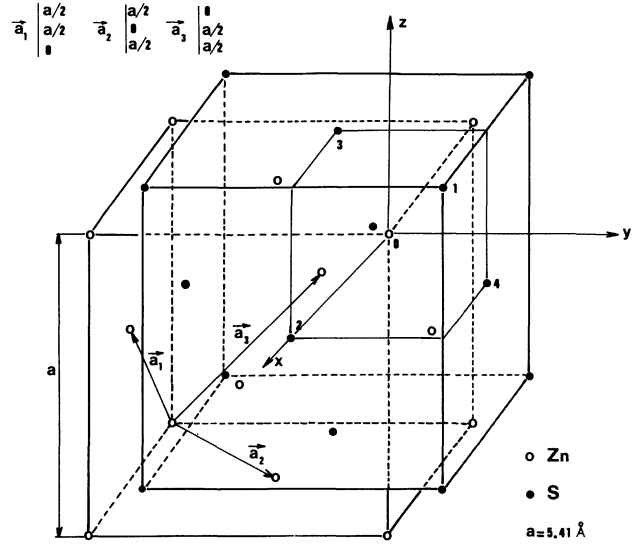


Fig. 2a. —  $S_1, S_2, S_3, S_4$  are the nearest neighbours of the Zn ion taken as origin (distance  $a\sqrt{3}/4$ ).

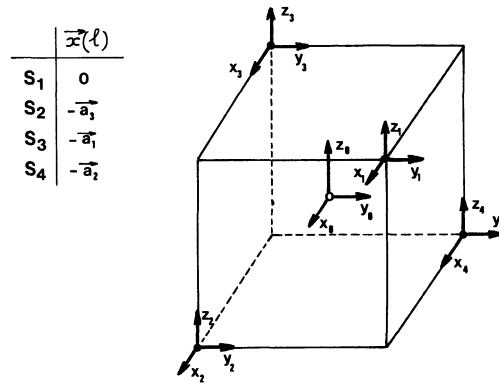


Fig. 2b. — Coordinates for atom displacements.

Under these conditions, for a crystal having  $N$  cells, the displacement of the atom on the  $(l, \kappa)$  site is :

$$\mathbf{u}(l, \kappa) = \sum_{\mathbf{k}j} \sqrt{\frac{\hbar}{2NM_\kappa \omega_j(\mathbf{k})}} \times \{ \mathbf{e}^*(\kappa | j) a_{\mathbf{k}j}^\dagger e^{-i\mathbf{k}\cdot\mathbf{x}(l)} + \mathbf{e}(\kappa | j) a_{\mathbf{k}j} e^{i\mathbf{k}\cdot\mathbf{x}(l)} \} . \quad (3)$$

In this expression  $a_{\mathbf{k}j}^\dagger$  is the creation operator for phonons belonging to the  $(\mathbf{k}j)$  mode ;  $j$  is the index for a branch of the dispersion curve,  $\omega_j(\mathbf{k})$  the frequency corresponding to the wave vector  $\mathbf{k}$  in the branch  $j$  and  $\mathbf{e}(\kappa | j)$  is the polarization vector of the  $(\mathbf{k}j)$  mode for a  $\kappa$  type atom.

The spin-phonon interaction is treated according to Van Vleck's method. The normal coordinates for the vibrations of the cluster mode of a paramagnetic ion with its nearest neighbours ( $T_d$  symmetry) are listed in table I if  $Q_l$  and  $Q_m$  are such coordinates and  $V$  the crystalline field potential created by the nearest

Table I. — Normal coordinates.

$$\begin{aligned}
A_1 \quad Q_{A_1} &= \frac{M_1}{12} (X_1 + X_2 - X_3 - X_4 + Y_1 - Y_2 - Y_3 + Y_4 + Z_1 - Z_2 + Z_3 - Z_4) \\
E \quad \left\{ \begin{aligned} Q_0 &= \frac{\sqrt{M_1}}{2\sqrt{6}} (X_1 + X_2 - X_3 - X_4 + Y_1 - Y_2 - Y_3 + Y_4 - 2(Z_1 - Z_2 + Z_3 - Z_4)) \\ Q_\varepsilon &= \frac{M_1}{2\sqrt{2}} (-(X_1 + X_2 - X_3 - X_4) + Y_1 - Y_2 - Y_3 - Y_4) \end{aligned} \right. \\
T_2^a \quad \left\{ \begin{aligned} Q_\xi^a &= \frac{\sqrt{M_1}}{2\sqrt{1 + 4\frac{M_1}{M_0}}} (X_1 + X_2 + X_3 + X_4 - 4X_0) \\ Q_\eta^a &= \frac{\sqrt{M_1}}{2\sqrt{1 + 4\frac{M_1}{M_0}}} (Y_1 + Y_2 + Y_3 + Y_4 - 4Y_0) \\ Q_\zeta^a &= \frac{\sqrt{M_1}}{2\sqrt{1 + 4\frac{M_1}{M_0}}} (Z_1 + Z_2 + Z_3 + Z_4 - 4Z_0) \end{aligned} \right. \\
T_2^b \quad \left\{ \begin{aligned} Q_\xi^b &= \frac{\sqrt{M_1}}{2\sqrt{2}} (Y_1 - Y_2 + Y_3 - Y_4 + Z_1 - Z_2 - Z_3 + Z_4) \\ Q_\eta^b &= \frac{\sqrt{M_1}}{2\sqrt{2}} (X_1 - X_2 - X_3 + X_4 + Z_1 + Z_2 - Z_3 - Z_4) \\ Q_\zeta^b &= \frac{\sqrt{M_1}}{2\sqrt{2}} (X_1 - X_2 - X_3 + X_4 + Y_1 + Y_2 - Y_3 - Y_4) \end{aligned} \right.
\end{aligned}$$

neighbours, the spin phonon interaction hamiltonian is

$$\mathcal{H}_{\text{SP}} = \sum_l \frac{\partial V}{\partial Q_l} Q_l + \frac{1}{2} \sum_{lm} \frac{\partial^2 V}{\partial Q_l \partial Q_m} Q_l Q_m.$$

Notations of [5] will be used throughout the following development. Then for a Raman process, the transition probability  $W_{M_S \rightarrow M_S - K}$  is expressed as a sum of terms having the form

$$E_{l'm'} = h_{lm} h_{l'm'}^* \sum_{jj'} \int \rho(\omega_j(\mathbf{k})) \rho(\omega_{j'}(\mathbf{k}')) q_{lv} q_{l'v}^* q_{mu} q_{m'u}^* \times d\Omega d\Omega' d\omega_j d\omega_{j'} \delta(\omega_j(\mathbf{k}) - \omega_{j'}(\mathbf{k}') + K\omega_0) \quad (4)$$

when only processes which are of 2nd order in  $\mathcal{H}_{\text{SP}}$  and 1st order in time dependent perturbation theory are included.

The  $h_{lm}$  are matrix elements of an operator acting on electronic states and the  $q_{lv}$  and  $q_{mu}$  are matrix elements of operators acting on lattice states. ( $v$  is an index for the absorption of one phonon and  $u$  for the emission of one phonon.)

The number of phonon states for a given value of  $\mathbf{k}$

(modulus and direction) in the solid angle  $d\Omega$  and the energy interval  $d\omega$  is  $\rho(\omega_j(\mathbf{k})) d\Omega d\omega$ , an expression which applies to the branch  $j$ .

For a real crystal, the calculation of such an expression is a considerable task. Therefore we introduce some approximations.

We firstly suppose that the dispersion curves  $\omega = \omega(\mathbf{k})$  are independent of the  $\mathbf{k}$  direction which is fairly well justified by Kunc's results [7], at least for the high symmetry directions. Then :

$$\begin{aligned}
E_{l'm'} = h_{lm} h_{l'm'}^* \left\{ \sum_{jj'} \int \rho[\omega_j(k)] \rho[\omega_{j'}(k')] \delta[\omega_j(k) - \omega_{j'}(k') + K\omega_0] \times \right. \\
\left. \times \left[ \int q_{lv} q_{l'v}^* d\Omega \int q_{mu} q_{m'u}^* d\Omega \right] d\omega_j d\omega_{j'} \right\}. \quad (5)
\end{aligned}$$

Neglecting  $K\omega_0$  compared to  $\omega_f(k)$  (justified in high temperature range) the conditions  $\omega_f(k) \approx \omega_f(k')$  allows us to separate the summation into a sum over acoustical phonon branches and a sum over optical phonon branches :

$$E_{l'm'} = E_{l'm'}^{AC} + E_{l'm'}^{OP} .$$

Therefore the terms to be calculated are those of the form :

$$\int q_{lu} q_{l'u}^* d\Omega = \int \langle N_u + 1 | Q_l | N_u \rangle \langle N_u | Q_{l'}^* | N_u + 1 \rangle d\Omega$$

and

$$\int q_{mv} q_{m'v}^* d\Omega = \int \langle N_v - 1 | Q_m | N_v \rangle \langle N_v | Q_{m'}^* | N_v - 1 \rangle d\Omega .$$

The  $Q$  coordinates are linear combinations of the components of the atomic displacements  $\mathbf{u}$  (see Table I).

In consequence we write

$$\int q_{lu} q_{l'u}^* d\Omega = v_{kj}^2 \overline{Q_{ll'}} .$$

and

$$\int q_{lv} q_{l'v}^* d\Omega = v_{kj}^2 \overline{Q_{ll'}} \quad (6)$$

where

$$v_{kj} = \sqrt{\frac{\hbar(N(\mathbf{k}j) + 1)}{2N\omega_j(k)}} , \quad v'_{kj} = \sqrt{\frac{\hbar N(\mathbf{k}j)}{2N\omega_j(k)}} .$$

At this stage it is customary to make use of certain hypotheses for the sake of simplification : long wavelength approximation (which is justified at low temperatures) [12] on one hand and homogeneous deformation on the other [2, 3, 4, 5].

Our method has been to calculate numerically the quantities  $\overline{Q_{ll'}}$  as a function of  $k$  without supposing homogeneous deformation. As regards the long wavelength approximation we have retained only the expression of the polarization vectors for the acoustical and the optical modes.

Furthermore, making use of a model with degenerate transverse branches we have plotted, the quantities  $Q_{ll'}^{L(\alpha)}$  and  $Q_{ll'}^{T(\alpha)} = Q_{ll'}^{T_1(\alpha)} + Q_{ll'}^{T_2(\alpha)}$  which are non zero ( $L, T_1, T_2$  are indexes for longitudinal and transverse polarizations). By comparing these curves it is apparent that the *orthogonality* properties of normal vibration modes [12] for calculations of integrals (6) are approximately verified in this model.

In the following we shall neglect the off diagonal terms. Eq. (5) is then expressed by

$$E_{l'm'}^{(\alpha)} = |h_{lm}|^2 \int (v_L^2 \rho_L^{(\alpha)} \overline{Q_{mm}^{L(\alpha)}} + v_T^2 \rho_T^{(\alpha)} \overline{Q_{mm}^{T(\alpha)}}) \times (v_L^2 \rho_L^{(\alpha)} \overline{Q_{ll}^{L(\alpha)}} + v_T^2 \rho_T^{(\alpha)} \overline{Q_{ll}^{T(\alpha)}}) d\omega . \quad (7)$$

Besides, we observe that those properties which have been established in connection with the approximations mentioned above and which, of course, apply to the  $A_1, E, T_2$  coordinates (*homogeneous deformations*) are almost retained here and that they apply as well for acoustical phonons as for optical phonons :

$$\begin{aligned} \overline{Q_{A_1 A_1}^{T(\alpha)}} &\approx 0 \quad (\text{we shall neglect the } Q_{A_1} \text{ contribution}) \\ \overline{Q_{\epsilon\epsilon}^{L(\alpha)}} &= \overline{Q_{\theta\theta}^{L(\alpha)}} = \overline{Q_{T_{2\xi}^a T_{2\xi}^a}^{L(\alpha)}} = \overline{Q_{T_{2\eta}^a T_{2\eta}^a}^{L(\alpha)}} = \overline{Q_{T_{2\xi}^b T_{2\xi}^b}^{L(\alpha)}} = \overline{Q_{T_{2\eta}^b T_{2\eta}^b}^{L(\alpha)}} \\ \overline{Q_{\epsilon\epsilon}^{T(\alpha)}} &= \overline{Q_{\theta\theta}^{T(\alpha)}} = \overline{Q_{T_{2\xi}^a T_{2\xi}^a}^{T(\alpha)}} = \overline{Q_{T_{2\eta}^a T_{2\eta}^a}^{T(\alpha)}} = \overline{Q_{T_{2\xi}^b T_{2\xi}^b}^{T(\alpha)}} = \overline{Q_{T_{2\eta}^b T_{2\eta}^b}^{T(\alpha)}} \end{aligned}$$

and the relation  $\overline{Q_T^{(\alpha)}} \neq \frac{3}{2} \overline{Q_L^{(\alpha)}}$  holds.

Moreover, the  $T_2^a$  coordinates, whose contribution is zero in the homogeneous approximation lead in our calculations to the following matrix elements :

$$\begin{aligned} \overline{Q_{T_{2\xi}^a T_{2\xi}^a}^{L(\alpha)}} &= \overline{Q_{T_{2\eta}^a T_{2\eta}^a}^{L(\alpha)}} = \overline{Q_{T_{2\xi}^b T_{2\xi}^b}^{L(\alpha)}} = \overline{Q_L^{(\alpha)}} \\ \overline{Q_{T_{2\xi}^a T_{2\xi}^a}^{T(\alpha)}} &= \overline{Q_{T_{2\eta}^a T_{2\eta}^a}^{T(\alpha)}} = \overline{Q_{T_{2\xi}^b T_{2\xi}^b}^{T(\alpha)}} = \overline{Q_T^{(\alpha)}} \end{aligned}$$

with  $\overline{Q_T^{(\alpha)}} \neq 2 \overline{Q_L^{(\alpha)}}$ .

It appears also that for coordinates relative to *homogeneous* deformations we have  $Q_{ll'}^{OP} = 2 Q_{ll'}^{AC}$  whereas the contributions of  $T_2^a$  type coordinates are

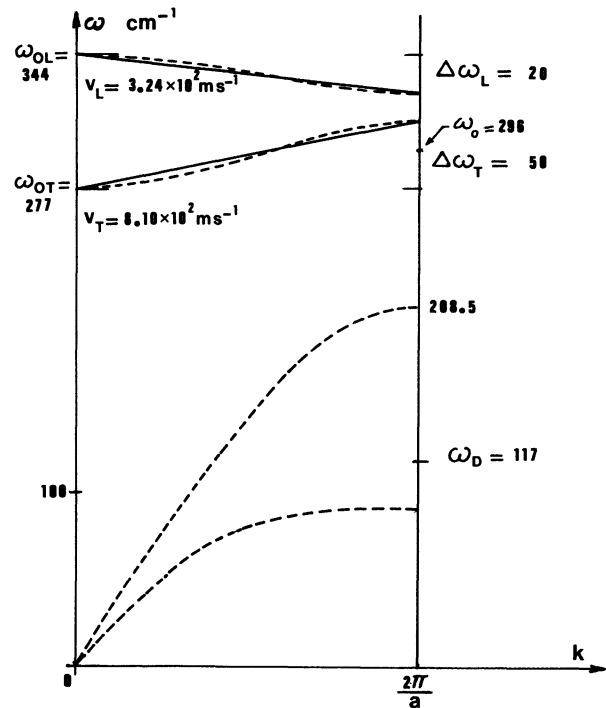


Fig. 3. — ZnS dispersion curves in  $|100|$  direction (from [6]) (dashed lines). The Debye approximations for optical branches are shown (solid lines).

radically different functions of  $k$  for acoustical or for optical modes.

Finally to within an excellent approximation these quantities may be expressed in the form of polynomial functions of  $k$

$$\begin{aligned}\overline{Q_{ll}^{AC}} &= a_0(l) + a_1(l) \left(\frac{a}{2}k\right)^2 + \\ &\quad + a_2(l) \left(\frac{a}{2}k\right)^4 + a_3(l) \left(\frac{a}{2}k\right)^6 \\ \overline{Q_{ll}^{OP}} &= b_0(l) + b_1(l) \left(\frac{a}{2}k\right)^2 + \\ &\quad + b_2(l) \left(\frac{a}{2}k\right)^4 + b_3(l) \left(\frac{a}{2}k\right)^6.\end{aligned}$$

The  $a_p$  and  $b_p$  coefficients are listed in table II.

In order to continue our numerical calculation of expressions (7) an approximation like the Debye approximation will be made for the dispersion curves  $\omega(k)$  of the optical branches. Using the curves reported

Table II.

	$a_0$	$a_1$	$a_2$	$a_3$
$\overline{Q_L^{AC}}$	0	$\frac{8 \Pi}{45}$	- 0.056 46	0.001 93
$\overline{Q_L'^{AC}}$	0	$\frac{4 \Pi}{27}$	- 0.044 054	0.001 462
$\overline{Q_L'^{OP}}$	$\frac{8 \Pi}{3}$	$-\frac{16 \Pi}{27}$	0.176 216	- 0.005 849

by Kunc for the  $|100|$  crystal direction we shall take the numerical values quoted in figure 3.

Introducing

$$V_{2n+3}(l) = \frac{1}{v_L^{2n+3}} + \frac{\delta(l)}{v_T^{2n+3}}$$

where  $v_L$  and  $v_T$  are velocities for acoustical modes (Debye approximation) with  $\delta(l) = 2$  if  $Q_l \in T_2^a$  and  $\delta(l) = 3/2$  in the opposite case then expression (7) leads to

$$E_{lm}^{AC} = \sum_{n,p=0}^3 |h_{lm}|^2 \left(\frac{\hbar V}{16 \pi^3 N}\right)^2 a_n(m) a_p(l) V_{2n+3}(m) V_{2p+3}(l) \int_0^{\omega_D} \langle N+1 \rangle \langle N \rangle \omega^{2(n+p+1)} d\omega. \quad (7')$$

In this expression  $\langle N \rangle$  is the mean phonon number for temperature  $T$  in the considered mode, at frequency  $\omega$ , and  $V$  is the sample volume. For optical branches, owing to the fact that the longitudinal band and the transverse bands (the latter being degenerate in our model) do not overlap, (7) is written :

$$E_{lm}^{OP} = |h_{lm}|^2 \left(\frac{\hbar V}{16 \pi^3 N}\right)^2 \sum_{n,p=0}^3 b_n(m) b_p(l) J_{n+p} \quad (7'')$$

where

$$\begin{aligned}J_{n+p} &= \frac{1}{v_L^{2(n+p+3)}} K_L(n, p) + \frac{\delta}{v_T^{2(n+p+3)}} K_T(n, p) \\ K_L(n, p) &= \int_{\omega_{OL} - \Delta\omega_L}^{\omega_{OL}} (\omega - \omega_{OL})^{2(n+p+2)} \langle N \rangle \langle N+1 \rangle \frac{d\omega}{\omega^2} \\ K_T(n, p) &= \int_{\omega_{OT}}^{\omega_{OT} + \Delta\omega_T} (\omega - \omega_{OT})^{2(n+p+2)} \langle N \rangle \langle N+1 \rangle \frac{d\omega}{\omega^2}\end{aligned}$$

$v_L$  and  $v_T$  are the longitudinal and the transverse optical wave velocity; if  $Q_l$  and  $Q_m \in T_2^a$ ,  $\delta = 4$ , if  $Q_l$  and  $Q_m \notin T_2^a$ ,  $\delta = 9/4$  but if  $Q_l \in T_2^a$  and  $Q_m \notin T_2^a$ ,  $\delta = 3$ .

As optical bandwidths are such that  $\Delta\omega \ll \omega_0$  the integrals  $K(n, p)$  can be written approximately :

$$K(n, p) = \frac{1}{2(n+p)+5} \cdot \frac{\Delta\omega^{2(n+p)+5}}{4 \text{sh}^2(\hbar\omega_0/2 kT)}. \quad (8)$$

In order to establish the comparative efficiency of the Raman processes resulting from acoustical phonons and from optical phonons the expressions (7') and (7'') will be evaluated in the high temperature limit where the Raman integrals and those of the formula (8) vary as  $T^2$ .

The quantities (7') will be calculated taking the numerical values used by Deville [5] :  $\theta_D = 168$  K and  $v_T = 2.5 \times 10^3$  m.s<sup>-1</sup>.  $\theta_D$  has been experimentally obtained by these authors and  $v_T$  is a mean value they deduced from calculated transverse velocities for different directions of propagation.

The ratio  $r = E_{lm}^{AC}/E_{lm}^{OP}$  is then calculated. It is found that

$$\begin{aligned}r &= 0.5 \quad \text{if } l, m \in T_2^a, \\ r &= 0.4 \quad \text{if } l, m \notin T_2^a, \\ r &= 0.6 \quad \text{if } l \notin T_2^a \text{ and } m \in T_2^a.\end{aligned}$$

It should be observed that the  $v_T$  value used here proceeds from long wave length calculations and that small variations of this quantity will result in noticeable

variations in  $r$ . So the results we obtain here must be considered only as an estimate of the order of magnitude.

**4. Conclusion.** — We have shown that the thermal variations of the reciprocal of the spin-lattice relaxation time for  $\text{Mn}^+$  in ZnS are in disagreement in the high temperature range with the law extrapolated from lower temperatures. This can be interpreted if the optical branches of phonons are taken into account and leads to an additional term in  $T_1^{-1}$  of the form

$$\beta \left| \text{sh}^2 \frac{h\omega_0}{2kT} \right|^{-1}.$$

This latter contribution is as important as that of the acoustical phonons.

Experimentally we find  $\omega_0 = 296 \text{ cm}^{-1}$  which is indeed in the frequency band occupied by the optical branches in ZnS. We also show by a numerical estimate that the contribution from the two kinds of phonons, acoustical and optical, are of the same order. This estimate required rather complex calculations since we made use neither of the long wavelength picture nor of the homogeneous deformation approximation.

### References

- [1] WAGNER, G. R., CASTLE, J. G., MURPHY, J., *II-VI Semiconducting compounds, International Conference, 1967* (D. G. Thomas, ed.) (W. A. Benjamin inc.) p. 1212.
- [2] DEVILLE, A., BLANCHARD, C., GAILLARD, B., GAYDA, J. P., *J. Physique* **36** (1975) 1151.
- [3] DEVILLE, A., BLANCHARD, C., GAILLARD, B., *J. Physique* **37** (1976) 1067.
- [4] BLANCHARD, C., DEVILLE, A., GAILLARD, B., *J. Physique* **37** (1976) 1475.
- [5] DEVILLE, A., Thèse d'Etat, Aix-Marseille I (1976), n° d'ordre C.N.R.S. A.O. 12214.
- [6] ABRAGAM, A., BLEANY, B., *Electron Paramagnetic Resonance of transition Ions* (Clarendon Press, Oxford) 1970, p. 574. DEVILLE *et al.*, have verified that this method and progressive saturation method led to the same value for  $T_1$  at 100 K in ZnS :  $\text{Fe}^{3+}$  (see ref. [10]).
- [7] KUNC, K., Thèse d'Etat, Paris VI (1973).
- [8] CHAO, YUAN-HUANG, *Phys. Rev.* **154** (1967) 215.
- [9] JELENSKI, A., SZYMCZAK, H., CJUTOMSKY, M., *J. Physique* **36** (1975) 1011.
- [10] DEVILLE, A., GAILLARD, B., BLANCHARD, C., LANDI, A., *Spin-lattice relaxation of  $\text{Fe}^{3+}$  in ZnS; experimental evidence of the optical phonons.* Submitted to *J. Physique*. BLANCHARD, C., GAILLARD, B., DEVILLE, A., *Relative importance of the  $T^{-5}$  and  $T^{-7}$  terms in spin-lattice relaxation time.* *J. Physique* **40** (1979) 1179.
- [11] MARADUDIN, A. A., MONTROLL, WEISS, G. H., *Theory of lattice dynamics in the harmonic approximation* (Academic Press, N.Y.) 1963.
- [12] VAN VLECK, J. H., *Phys. Rev.* **57** (1940) 426.